Experimental evidence of correlation between 1/f noise level and metal-to-insulator transition temperature in epitaxial La0.7Sr0.3MnO3 thin films

Laurence Méchin, Sheng Wu, Bruno Guillet, Paolo Perna, Cédric Fur, Sylvain Lebargy, C. Adamo, D.G. Schlom, Jean-Marc Routoure

FAST TRACK COMMUNICATION

Experimental evidence of correlation between $1/f$ noise level and metal-to-insulator transition temperature in epitaxial $La_{0.7}Sr_{0.3}MnO_3$ thin films

L Méchin[1], S Wu[1], B Guillet[1], P Perna[1,2], C Fur[1], S Lebargy[1], C Adamo[3], D G Schlom[3,4] and J M Routoure[1]

[1] GREYC (UMR 6072) CNRS ENSICAEN Université de Caen Basse-Normandie, 14050 Caen cedex, France
[2] Instituto Madrileño de Estudios Avanzados en Nanociencia, IMDEA-Nanociencia, Campus Universidad Autónoma de Madrid, 28049 Madrid, Spain
[3] Department of Materials Science and Engineering, Cornell University, Ithaca, NY 14853-1501, USA
[4] Kavli Institute at Cornell for Nanoscale Science, Ithaca, NY 14853, USA

Abstract

The relation between lattice deformation, dc electrical properties and $1/f$ noise at room temperature was investigated experimentally in two series of high epitaxial $La_{0.7}Sr_{0.3}MnO_3$ (LSMO) thin films of various thicknesses. The first series was deposited on $SrTiO_3$ (0 0 1) single crystal substrates by pulsed laser deposition and the second one on $SrTiO_3$-buffered Si (0 0 1) substrates by reactive-molecular-beam epitaxy. A clear correlation was found between $1/f$ noise level and the temperature of the metal-to-insulator transition. These findings are important in view of the optimization of LSMO thin films for applications in sensors.

$La_{0.7}Sr_{0.3}MnO_3$ (LSMO) is a ferromagnetic oxide showing a ferromagnetic-to-paramagnetic transition at a Curie temperature T_C of about 360 K accompanied by a metal-to-insulator transition occurring at T_{MI} (the temperature of the metal-to-insulator transition, where the electrical resistance is maximum). Interestingly the maximum of the derivative of electrical resistance versus temperature occurs at temperatures below T_C, i.e. close to room temperature, giving rise to potential room temperature thermometric and bolometric applications [1–4]. For any kind of sensor, noise level has to be considered in addition to the above cited remarkable properties [5]. Despite previous studies on electronic noise in magnetic materials [6] and more specifically manganites [7], no clear conclusions are given about the physical origin of low-frequency noise in LSMO [8–13]. It should be noted that noise measurements in the literature have been carried out under a variety of conditions and geometries on samples with different structural properties. This can explain why it is often difficult to compare data. The main conclusion that may be drawn from existing studies on epitaxial thin films, polycrystals or crystals is that the noise level depends on the structural quality of the tested samples and that it is affected by the presence of oxygen vacancies. It was also shown that lattice mismatch between films and substrates significantly influenced the noise level [14]. Further, the origin of low-frequency noise in materials and devices can hardly be predicted.

With the goal of experimentally correlating the $1/f$ noise level of LSMO thin films with structural (strain and lattice deformation) and dc electrical properties (room temperature electrical resistivity and T_{MI}) on a large number of LSMO

Table 1. Summary of the structural parameters of the LSMO films, where c_{LSMO} and c_{STO} are the measured out-of-plane lattice parameter of LSMO and STO, respectively, and $\varepsilon_{[0\,0\,1]}$ is the LSMO out-of-plane lattice deformation.

Material	Film thickness (nm)	FWHM of the 0 0 2 peak in $\theta - 2\theta$ scans (°)	FWHM of the 0 0 2 peak in ω-scans (°)	rms roughness in $1\times1\ \mu m^2$ AFM images (nm)	c_{LSMO} or c_{STO} (nm)	$\varepsilon_{[0\,0\,1]}$ (%)
LSMO/STO series						
LSMO	5	>1.10	Not measurable	—	0.3834	−1.00
	8	1.10	Not measurable	0.29	0.3843	−0.78
	20	0.31	0.16	0.15	0.3855	−0.47
	40	0.20	0.19	0.19	0.3851	−0.57
	75	0.11	0.18	0.18	0.3854	−0.48
	120	0.08	0.14	0.13	0.3855	−0.46
LSMO/STO/Si series						
LSMO	10	0.41	0.33	0.59	0.3838	−0.91
	20	0.31	0.29	0.42	0.3839	−0.87
	60	0.16	0.22	0.50	0.3848	−0.65
	75	0.12	0.18	0.57	0.3849	−0.62
	100	0.10	0.26	0.96	0.3853	−0.52
STO	20	0.45	0.39	—	0.3894	—

samples from different origins and of various thicknesses, we studied two different series of LSMO films, deposited either on single crystal $SrTiO_3$ (STO) (0 0 1) substrates by pulsed laser deposition (PLD) or on STO-buffered Si (0 0 1) substrates by reactive molecular-beam-epitaxy (MBE). Some of the properties of the LSMO/STO/Si samples have already been published in [15]. The two series of films showed different lattice mismatch between LSMO and STO depending on whether the STO was in bulk or thin film form, while keeping LSMO films of high epitaxial quality. After a brief description of the deposition conditions, the structural and dc electrical properties are given for all films. The $1/f$ noise level measurements at room temperature are then described. We finally consider possible correlations between lattice deformation, dc electrical properties, T_{MI}, and $1/f$ noise level.

As encountered in many other transition metal oxides a strong correlation between structural and physical (magnetic or electric) properties can be observed in LSMO. The strain in epitaxial thin films can be controlled by an appropriate choice of substrates. Thanks to the lattice mismatch δ between the in-plane lattice parameters of a film (a_{film}) and the substrate ($a_{substrate}$) it is epitaxially grown on defined as [16]

$$\delta = \frac{a_{substrate} - a_{film}}{a_{substrate}}, \qquad (1)$$

one can induce either in-plane tensile or compressive strain if $\delta > 0$ or <0, respectively. Bulk LSMO exhibits hexagonal, orthorhombic or rhombohedral perovskite structures. When prepared in the form of epitaxial thin films on well matched crystalline substrates such as cubic STO (with $a_{STOc} = c_{STOc} = 0.3905$ nm), its crystallographic structure differs from that of the bulk to become pseudo-cubic (with $a_{LSMOpc} = c_{LSMOpc} = 0.3873$ nm), where a and c are the in-plane and out-of-plane lattice parameters, respectively [17]. The effects of strain on magnetic and electrical properties have been studied by varying the substrate lattice constant [18–24]. Particular substrate orientations such as (1 1 0) or vicinal cuts have also been used to control the magnetic anisotropy and the magnetization reversal mechanism [25, 26].

In the case of epitaxial films, varying film thickness is an easy way to vary the average strain. In the case of thin film growth on relatively well matched substrates, such as STO (0 0 1) substrates for LSMO, fully strained (commensurate) and partially relaxed regimes are commonly observed, depending on whether the film thickness is smaller or higher than a critical thickness. This critical thickness for LSMO thin films grown on STO (0 0 1) substrates is in the 60–150 nm range depending on the deposition conditions and system used [27–30]. Above this critical thickness the c parameter increases to be closer to the bulk LSMO value, revealing partially relaxed LSMO films in which the strain is inhomogeneous. Maurice *et al* made a comprehensive study about the evolution of the LSMO lattice parameters with film thickness [29]. A tetragonal distortion of the lattice was observed over the whole thickness range and, remarkably, above 100 nm a significant proportion of the LSMO keeps the fully strained parameters, while the other part adopts a less tetragonal unit cell [31]. Such bimodal relaxation is common in partially relaxed epitaxial films [32–34]. The c parameter never reached the bulk c value. Maurice *et al* [29] also showed that the magnetic properties of the LSMO thin films are close to those of bulk LSMO, but degraded in partially relaxed films.

The LSMO thin films studied were deposited on STO (0 0 1) substrates by PLD at 720 °C in a O_2 pressure of 0.26 Torr (i.e., 34.7 Pa), and on 20 nm thick STO-buffered Si (0 0 1) substrates by reactive MBE at 670 °C in a distilled ozone background pressure of 5×10^{-7} Torr (i.e., 6.7×10^{-5} Pa). More details on the deposition conditions of the LSMO/STO/Si samples can be found in [15, 23, 35]. The LSMO thickness was varied from 5 to 150 nm on the STO substrates and from 10 to 100 nm on the STO/Si substrates. The thickness was first targeted using the number of pulses for PLD and the growth time for MBE, and it was *a posteriori* checked using x-ray reflectivity. The two series of LSMO films showed very comparable structural properties (see table 1). X-ray diffraction patterns in the $\theta - 2\theta$ configuration using Bragg–Brentano geometry and CuK_α radiation were performed. All LSMO films were (0 0 1) oriented as seen in figure 1. Reciprocal space maps of regions around the 1 0 3, 1 1 3, 1 1 3

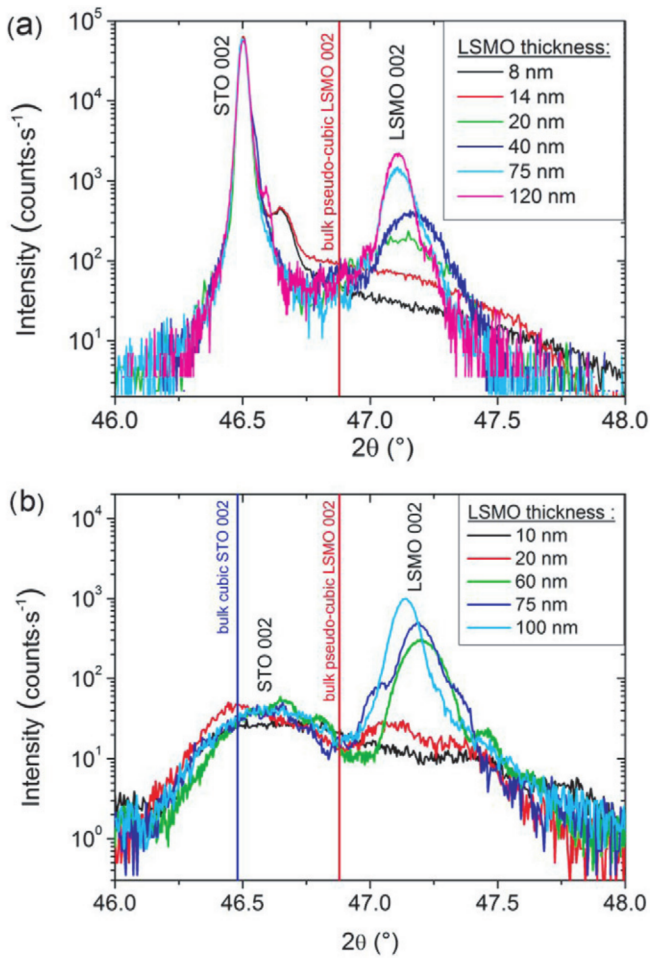

Figure 1. X-ray diffraction patterns in the $\theta - 2\theta$ configuration of LSMO films of various thicknesses deposited (*a*) on STO (0 0 1) substrates and (*b*) on STO/Si (0 0 1) substrates.

and 3 0 3 peaks performed on LSMO/STO samples deposited under similar conditions as the one presented here confirmed the epitaxy of LSMO on STO (0 0 1) substrates with an orientation relationship of (0 0 1) LSMO//(0 0 1) STO and [1 0 0] LSMO//[1 0 0] STO. A pole figure of the 1 0 1 peak of the 60 nm thick LSMO/STO/Si sample also showed that it was epitaxially grown with an orientation relationship of (0 0 1) LSMO//(0 0 1) STO//(0 0 1) Si and [1 0 0] LSMO//[1 0 0] STO//[1 1 0] Si. The full-width at half-maximum (FWHM) of the 0 0 2 LSMO peak in the ω-scan configuration did not vary very much, from 0.33° at thickness below 10 nm down to about 0.14–0.26° at 100–120 nm thickness, which can be considered as small values. Root mean square (rms) roughness measured by atomic force microscopy (AFM) did not vary significantly with LSMO film thickness, except for a small increase for the 100 nm thick LSMO film on STO/Si.

It is very important for our noise study that all LSMO films are of comparable structural quality, so that we can study the influence of lattice deformation and other dc electrical properties in high quality films. The out-of-plane lattice parameter c_{LSMO} of LSMO films deposited on STO and on STO/Si, and c_{STO} of STO deposited on silicon is also reported in table 1. The measured c_{STO} value of STO was 0.3894 nm for all LSMO/STO/Si films, which gives $\delta = 0.54\%$ (to be compared with $\delta = 0.82\%$ when LSMO is deposited on STO substrates). The lattice mismatch between LSMO and the substrate is smaller for growth on STO/Si than for growth on STO. As expected from the positive δ values between LSMO and STO in both series of samples, LSMO films are strained showing an out-of-plane lattice parameter smaller than the bulk value (i.e. an in-plane tensile strain). From the c_{LSMO} values we determined the LSMO out-of-plane lattice deformation $\varepsilon_{[0\,0\,1]}$ defined as

$$\varepsilon_{[0\,0\,1]} = \frac{c_{\mathrm{LSMO}} - c_{\mathrm{LSMOpc}}}{c_{\mathrm{LSMOpc}}}, \tag{2}$$

where c_{LSMO} is the film out-of-plane lattice parameter, and c_{LSMOpc} is the pseudo-cubic lattice parameter of bulk LSMO (0.3873 nm) [16]. $\varepsilon_{[0\,0\,1]}$ is negative for the whole film thickness range (table 1).

Dc electrical resistivity measurements as a function of temperature were carried out on unpatterned films using the standard four-probe technique. Figure 2 shows the electrical resistivity versus temperature curves measured on all LSMO films. The measured electrical resistivity values were in the 1.4–3.8 mΩ cm range at 300 K for all the LSMO thicknesses above 8 nm (see table 2), which is very close to the bulk value [36]. Only the 5 nm thick LSMO film on STO showed a higher electrical resistivity of 10.6 mΩ cm, which is consistent with another study of the electrical transport in ultrathin LSMO films [37]. All films showed a metal-to-insulator transition temperature T_{MI} in the 337–390 K range (see the inset of figures 2(*a*) and (*b*)).

Noise measurements at room temperature were carried out on 20 and 50 μm wide microbridges of various lengths (50, 100, and 150 μm) patterned on each film in order to have well-defined volumes and to be able to average the noise values over several geometries. Standard UV photolithography followed by argon ion etching was used. Gold metal pads were fabricated using ion beam deposition and chemical etching in a KI solution. The 4 probe technique, a low noise home-made amplifier with a gain of 1000 and a spectrum analyser were used for electrical noise measurements at 300 K. With the additional use of a quasi-ideal dc current source, we checked that the contribution of parasitic contact noise can be neglected. Under these conditions the measured noise can be attributed to the LSMO film noise. Noise spectra typically consist of two parts: a low-frequency noise that depends on the bias current and the frequency, and the white part that is bias current and frequency independent. No Lorentzian component was observed. The voltage noise spectral density of the latter component is equal to $4k_{\mathrm{B}}TR$, where k_{B} is the Boltzmann constant, T is the temperature and R is the sample electrical resistance. We used the semi-empirical Hooge relation to describe the low-frequency noise in our samples [38]:

$$\frac{S_V}{V^2} = \frac{\alpha_{\mathrm{H}}}{n} \times \frac{1}{\Omega \times f}, \tag{3}$$

where S_V is the voltage noise spectral density ($\mathrm{V^2\,Hz^{-1}}$), V is the sample voltage (V), α_{H} is the Hooge parameter (dimensionless), n is the charge carrier concentration ($\mathrm{m^{-3}}$),

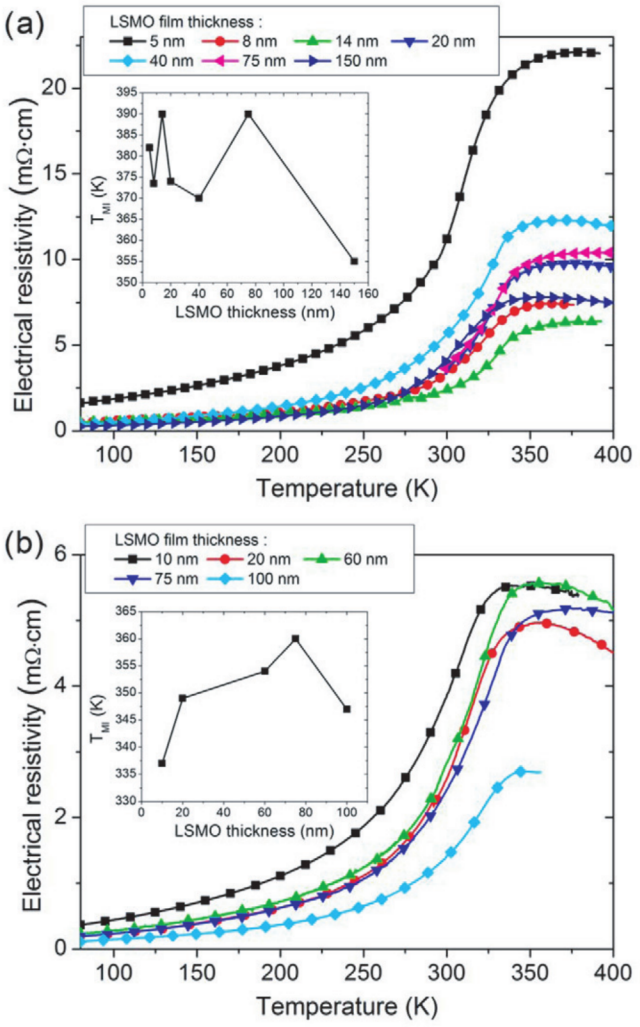

Figure 2. Electrical resistivity versus temperature characteristics of unpatterned LSMO films of various thicknesses deposited (*a*) on STO (0 0 1) substrates and (*b*) on STO/Si (0 0 1) substrates. Insets show the variation of T_{MI} with the LSMO film thickness.

Ω is the sample volume (m^3) and f is the measuring frequency (Hz). α_H/n is defined as the normalized Hooge parameter and is expressed in (m^3).

After the quadratic dependence of S_V with the sample voltage was checked we could calculate the normalized Hooge parameter α_H/n. For each film thickness the reported α_H/n values reported in table 2 are averaged over several 20 and 50 μm wide microbridges of various lengths (50, 100, or 150 μm). α_H/n varied from 2.36×10^{-31} to 3.41×10^{-30} m^3, which is among the lowest values reported for epitaxial LSMO films on STO (0 0 1) substrates, thus reaffirming the high quality of all the tested LSMO films [7, 10]. We observed that the $1/f$ noise level in LSMO is slightly lower on STO substrates than on STO/Si substrates.

Figure 3 shows the dependence of the measured normalized Hooge parameter on the LSMO out-of-plane deformation, the electrical resistivity at 300 K, and the temperature of metal-to-insulator transition. Among the investigated samples, the $1/f$ noise level showed no strong correlation with $\varepsilon_{[0\,0\,1]}$ or electrical resistivity at 300 K. Low quality epitaxial films, as judged by high FWHM of the 0 0 2 LSMO peak in the ω-scan configuration (about 1°), usually do show higher $1/f$ noise associated with an increase in the electrical resistivity at 300 K as previously shown for LSMO films deposited on yttria–stabilized–zirconia based buffered silicon substrates [39]. In this study, all films, except the 5 nm thick LSMO/STO, showed electrical resistivity values in the 1.4–4.5 mΩ cm range, i.e. varying by a factor of 3 at maximum, while α_H/n varied by about one order of magnitude at maximum with no common tendency. One can, however, observe a clear correlation of α_H/n with T_{MI} as is evident in figure 3(*c*). Interestingly, films showing the highest T_{MI} values also show the lowest noise level, following a quasi-linear dependence in the semi-log plot. This result could help us to find some indications about the origin of $1/f$ noise in LSMO thin films. A wide range of results on low-frequency noise in LSMO thin films, which are sometimes contradictory, can be found in the literature indeed [6–14]. It can be explained by the wide variety of sample geometries and structural properties. No affirmative conclusion about the origin of electrical noise in LSMO can be found. It could be of electric, magnetic or structural origin, or even a combination of them. Our study shows that $1/f$ noise level can vary by one order of magnitude while other structural properties are very similar. It therefore excludes a large contribution of the structural origin of $1/f$ noise in our epitaxially grown LSMO films. In contrast, thanks to the large number of measurements carried out on a large number of similar samples the experimental correlation between low-frequency noise and T_{MI} is evidenced. The dependence of T_{MI} with grain size [40] and oxygen vacancies [41] has been studied in LSMO thin films. It is generally found that T_{MI} increases when the grain size increases, i.e. when intragrain conduction dominates (the properties being closer to those of bulk LSMO) [40]. Orgiani *et al* [41] have systematically studied the effect of oxygen vacancies and correlated it to T_{MI}. Increasing the annealing time in vacuum, i.e. increasing oxygen vacancies, had the effect of reducing T_{MI}. Even if the studies by Liu *et al* [40] and Orgiani *et al* [41] concerned films of very different quality (polycrystalline and epitaxial films in the first case, or with T_{MI} varying in the 230–350 K range in the latter case), their conclusions added to our findings on the $1/f$ noise level correlation with T_{MI}, could indicate that $1/f$ noise in LSMO thin films is very dependent on grain size or oxygen vacancies. Further investigation is needed to definitively conclude.

In conclusion, structural, dc electrical transport properties, and $1/f$ noise level have been systematically studied for two series of LSMO films of high epitaxial quality, deposited on STO (0 0 1) and on STO/Si (0 0 1) substrates. Electrical resistivity at 300 K and lattice deformation appear not to be related to noise level. In contrast, T_{MI} seems to vary consistently with noise level, since high T_{MI} correspond to low noise and vice versa. Our results also show how noise can be a very sensitive indicator of film quality since care was taken in order to compare films with comparable structural properties. In view of sensor applications, where noise has to be considered as a critical parameter, we experimentally

Table 2. Summary of the electrical properties of the LSMO thin films.

Series	Film thickness (nm)	T_{MI} (K)	ρ at 300 K (mΩ cm)	α_H/n at 300 K (m^3)
LSMO/STO	5	382	10.6	$(7.36 \pm 0.99) \times 10^{-31}$
	8	374	3.2	$(3.44 \pm 0.38) \times 10^{-31}$
	14	390	2.3	$(2.36 \pm 0.24) \times 10^{-31}$
	20	374	3.6	$(3.71 \pm 0.52) \times 10^{-31}$
	40	370	1.8	$(2.47 \pm 0.59) \times 10^{-31}$
	75	390	2.9	—
	100	—	3.7	$(1.45 \pm 0.29) \times 10^{-30}$
	150	355	3.9	$(2.47 \pm 0.44) \times 10^{-30}$
LSMO/STO/Si	10	337	3.8	$(3.41 \pm 0.71) \times 10^{-30}$
	20	349	2.6	$(1.62 \pm 0.32) \times 10^{-30}$
	60	354	2.8	$(0.95 \pm 0.25) \times 10^{-30}$
	75	360	2.4	$(1.73 \pm 0.48) \times 10^{-30}$
	100	347	1.4	$(2.75 \pm 0.58) \times 10^{-30}$

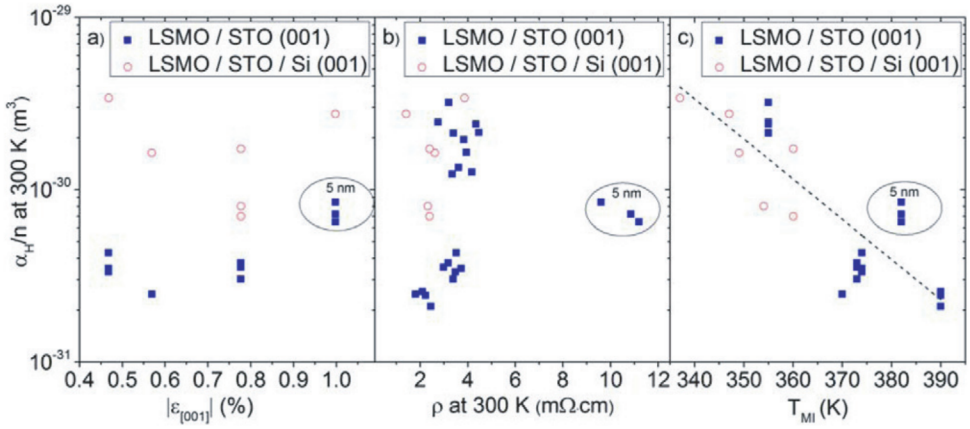

Figure 3. Summary of the dependence of the normalized Hooge parameter on the LSMO out-of-plane deformation, the electrical resistivity at 300 K and the temperature of the metal-to-insulator transition. The dashed line in figure 3(*c*) is a linear fit of all data in the semi-log plot.

showed that measuring the T_{MI} values already gives a good indication of the final noise level that can be expected in a device.

Acknowledgments

The work at Cornell was supported by AFOSR through award No FA9550-10-1-0524. P P acknowledges support through the Marie Curie AMAROUT EU action and the Spanish MICINN 'Juan de la Cierva' contract.

References

[1] Venkatesan T, Rajaswari M, Dong Z, Ogale S B and Ramesh R 1998 *Phil. Trans. R. Soc. Lond.* A **356** 1661
[2] Goyal A, Rajeswari M, Shreekala R, Lofland S E, Bhagat S M, Boettcher T, Kwon C, Ramesh R and Venkatesan T 1997 *Appl. Phys. Lett.* **71** 2535
[3] Méchin L, Routoure J M, Guillet B, Yang F, Flament S, Robbes D and Chakalov R A 2005 *Appl. Phys. Lett.* **87** 204103
[4] Yang F, Méchin L, Routoure J M, Guillet B and Chakalov R A 2006 *J. Appl. Phys.* **99** 024903
[5] Fadil D *et al* 2012 *J. Appl. Phys.* **112** 013906
[6] Raquet B 2001 Electronic noise in magnetic material and devices *Spin Electronics* ed M Ziese and M J Thornton (Berlin: Springer) pp 232–73
[7] Méchin L, Routoure J-M, Mercone S, Yang F, Flament S and Chakalov R A 2008 *J. Appl. Phys.* **103** 083709
[8] Raquet B, Coey J M D, Wirth S and von Molnar S 1999 *Phys. Rev.* B **59** 12435
[9] Lisauskas A, Khartsev S I and Grishin A M 1999 *J. Low Temp. Phys.* **117** 1647
[10] Palanisami A, Merithew R D, Weissman M B, Warusawithana M P, Hess F M and Eckstein J N 2002 *Phys. Rev.* B **66** 092407
[11] Han K-H, Huang Q, Ong P C and Ong C K 2002 *J. Phys.: Condens. Matter.* **14** 6619
[12] Barone C, Adamo C, Galdi A, Orgiani P, Petrov A Yu, Quaranta O, Maritato L and Pagano S 2007 *Phys. Rev.* B **75** 174431
[13] Barone C, Pagano S, Méchin L, Routoure J-M, Orgiani P and Maritato L 2008 *Rev. Sci. Instrum.* **79** 053908
[14] Reutler P, Bensaid A, Herbstritt F, Höfener C, Marx A and Gross R 2000 *Phys. Rev.* B **62** 11619
[15] Méchin L, Adamo C, Wu S, Guillet B, Lebargy S, Fur C, Routoure J-M, Mercone S, Belmeguenai M and Schlom D G 2012 *Phys. Status Solidi* a **209** 1090
[16] Matthews J W 1975 *Epitaxial Growth, Part B* ed J W Matthews (New York: Academic) pp 559–609
[17] Hammouche A, Siebert E and Hammou A 1989 *Mater. Res. Bull.* **24** 367
[18] Millis A J, Darling T and Migliori A 1998 *J. Appl. Phys.* **83** 1588
[19] Tsui F, Smoak M C, Nath T K and Eom C B 2000 *Appl. Phys. Lett.* **76** 2421

[20] Berndt L M, Balbarin V and Suzuki Y 2000 *Appl. Phys. Lett.* **77** 2903
[21] Ziese M, Semmelhack H C and Han K H 2002 *J. Appl. Phys.* **91** 9930
[22] Steenbeck K and Habisreuther T, Dubourdieu C and Senateur J P 2002 *Appl. Phys. Lett.* **80** 3361
[23] Adamo C *et al* 2009 *Appl. Phys. Lett.* **95** 112504
[24] Boschker H, Mathews M, Brinks P, Houwman E, Vailionis A, Koster G, Blank D H A and Rijnders G 2011 *J. Magn. Magn. Mater.* **323** 2632
[25] Suzuki Y, Hwang H Y, Cheong S-W, Siegrist T, van Dover R B, Asamitsu A and Tokura Y 1998 *J. Appl. Phys.* **83** 7064
[26] Perna P, Rodrigo C, Jiménez E, Teran F J, Mikuszeit N, Méchin L, Camarero J and Miranda R 2011 *J. Appl. Phys.* **110** 013919
[27] Wiedenhorst B, Höfener C, Lu Y, Klein J, Alff L, Gross R, Freitag B H and Mader W 1999 *Appl. Phys. Lett.* **74** 3636
[28] Abrutis A, Plausinaitiene V, Kubilius V, Teiserskis A, Saltyte Z, Butkute R and Senateur J P 2002 *Thin Solid Films* **413** 32
[29] Maurice J-L, Pailloux F, Barthélémy A, Durand O, Imhoff D, Lyonnet R, Rocher A and Contour J-P 2003 *Phil. Mag.* **83** 3201
[30] Angeloni M, Balestrino G, Boggio N G, Medaglia P G, Orgiani P and Tebano A 2004 *J. Appl. Phys. Lett.* **96** 6387
[31] Biegalski M D *et al* 2008 *J. Appl. Phys.* **104** 114109
[32] Miceli P F and Palmstrøm C J 1995 *Phys. Rev.* B **51** 5506
[33] Kim C, Robinson I K, Spila T and Greene J E 1998 *J. Appl. Phys.* **83** 7608
[34] Kortan A R, Hong M, Kwo J, Mannaerts J P and Kopylov N 1999 *Phys. Rev.* B **60** 10913–8
[35] Warusawithana M P *et al* 2009 *Science* **324** 367
[36] Urushibara A, Moritomo Y, Arima T, Asamitsu A, Kido G and Tokura Y 1995 *Phys. Rev.* B **51** 14103
[37] Boschker H, Kautz J, Houwman E P, Siemons W, Blank D H A, Huijben M, Koster G, Vailionis A and Rijnders G 2012 *Phys. Rev. Lett.* **109** 157207
[38] Hooge F N 1969 *Phys. Lett.* **29A** 139
[39] Méchin L, Perna P, Barone C, Routoure J-M and Simon Ch 2007 *Mater. Sci. Eng.* B **144** 73
[40] Liu X, Jiao Z, Nakamura K, Hatano T and Zeng Y 2000 *J. Appl. Phys.* **87** 2431
[41] Orgiani P, Petrov A Yu, Ciancio R, Galdi A, Maritato L and Davidson B A 2012 *Appl. Phys. Lett.* **100** 042404